Scientific Investigations Map 3451

CORRELATION OF MAP UNITS

[See Description of Map Units for precise unit ages]

PROTEROZOIC IGNEOUS

AND METAMORPHIC ROCKS

containing a matrix of finer rock fragments. Lower part of unit locally

contains interstitial ice, ice lenses, or an ice core. Rock fragments on and

within rock-glacier deposits are primarily derived from steep slopes and

upslope cliffs chiefly by rockfall and locally by rockslide and avalanche.

Colorado are of latest Pleistocene or early Holocene age (Meierding and

Orientations of curvilinear ridges and gullies on rock-glacier deposits

indicate downslope motion. Most of the rock-glacier deposits in

<sup>10</sup>Be Age Rel. Unc. Rel. Unc. <sup>26</sup>Al Age Rel. Unc. Rel. Unc. <sup>26</sup>Al Age/

(ka) (int) (ext) (ka) (int) (ext) <sup>10</sup>Be Age

MESOPROTEROZOIC AND

AND METAMORPHIC ROCKS

PALEOPROTEROZIC IGNEOUS

GLACIAL AND

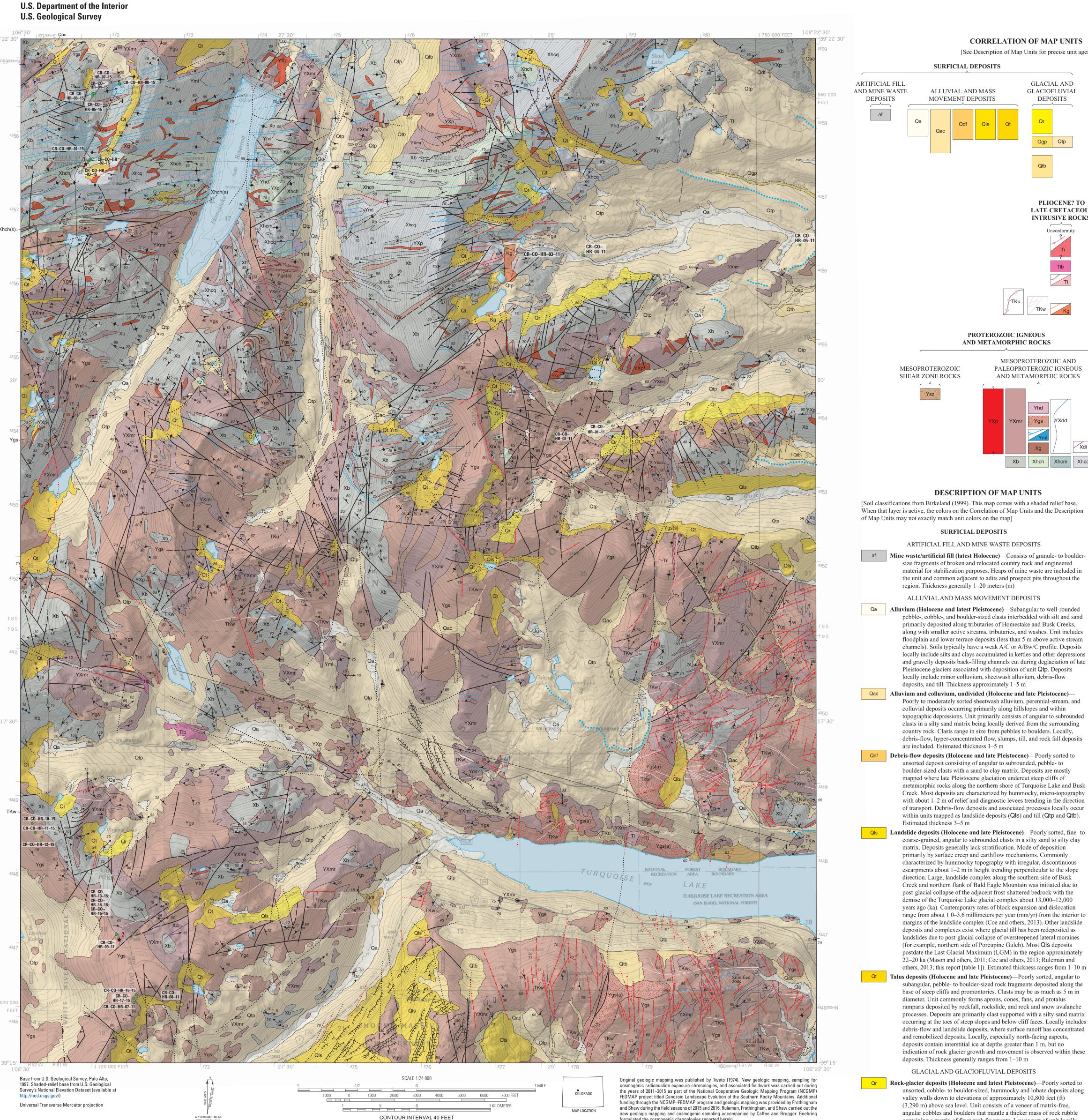
GLACIOFLUVIAL

DEPOSITS

PLIOCENE? TO

LATE CRETACEOUS

INTRUSIVE ROCKS



NATIONAL GEODETIC VERTICAL DATUM OF 1929

Dashed blue line shows the inferred Last Glacial Maximum (Pinedale Glaciation) ~22-20 thousand years ago (ka). Elevations and ice-covered bedrock knolls indicated by both field evidence and cosmogenic nuclide dating of glacially scoured bedrock surfaces and deposits

[Latitude and longitude in North American Datum 1927 (NAD 27); dd N, decimal degrees west; m, meters; cm, centimeters per year; E+, exponential base 10; mg, milligrams; Be, beryllium; qtz, quartz; g, grams; conc., concentration; std., standard; Al, aluminum; ka, thousands of years (kilo-annum); int, interior; ext, exterior; %, percent; --, no data]

Latitude Longitude Elevation Thickness Density Shielding Erosion rate Be carrier Mass qtz

| OBe/9Be | Error | OBe | OBe

<sup>10</sup>Be chronologies reported for the upper Arkansas River valley and central Colorado (Guido and others, 2007; Briner, 2009; Ward and others, 2009; and Young and others, 2011) when adjustments for production rates are made.

 $(dd\ N) \qquad (dd\ W) \qquad (m) \qquad (g/cm^2) \quad correction \quad (cm/yr) \qquad (mg) \qquad (g) \qquad (\times 10^{-15}) \qquad (atoms) \qquad (atoms) \qquad (atoms/g) \qquad (atoms/g)$ 

 $\text{CR-CO-HR-07-15} \quad 39.3695 \quad 106.4851 \quad 3,450 \quad 3 \quad 2.73 \quad 0.99 \quad 0.00 \quad 0.2696 \quad 30.306999206543 \quad 1,175.81 \quad 19.6695 \quad 2.12E+07 \quad 3.54E+05 \quad 6.98E+05 \quad 1.17E+04 \quad 07KNSTD \quad 1,506.95 \quad 1.17E+04 \quad 0.98E+05 \quad 0.98E+05$ 

Photograph 2. View to the west-southwest of the Continental Divide and the Fryingpan-Roaring Fork watershed from Hagerman Pass (11,925 feet above sea level [asl]; 3,635 meters asl). Ft, feet; m, meter. Photograph by C.A. Ruleman, 2015.

For more information concerning this publication, contact

To learn about the USGS and its information products visit

Box 25046, Mail Stop 980

https://www.usgs.gov/centers/gecsc

For product and ordering information visit

enter Director, USGS Geosciences and Environmental Change Science Center

Or visit the Geosciences and Environmental Change Science Center Web site at

Table 1. 10 Be and 26 Al cosmogenic radionuclide sample data and age analyses. Sampling was carried out following established procedures outlined in Gosse and Phillips (2001). This included recording elevation, latitude, longitude, and top ographic shielding data for each samples were

calculated using the CRONUS-Earth online calculator ver. 2.2, following the time-invariant scaling model of Lal (1991) and Stone (2000). Uncertainties are reported at the 1 sigma level (σ) (about 9 percent external uncertainty; Balco and others, 2008). Consistent with past studies within the region, no corrections for erosion or snow cover were applied, which allows for comparison with previous

 $\text{CR-CO-HR-05-11} \quad 39.35169 \quad 106.378 \quad 3,304 \quad 3 \quad 2.73 \quad 1.00 \quad 0.00 \quad 0.288 \quad 19.597 \quad 662.779 \quad 16.1912 \quad 1.27E+07 \quad 3.12E+05 \quad 6.47E+05 \quad 1.59E+04 \quad 07KNSTD \quad 1,774.11 \quad 69.9893 \quad 8.24E+07 \quad 3.25E+06 \quad 4.20E+06 \quad 1.66E+05 \quad KNSTD \quad 6.50025502609462 \quad 15,502 \quad 382 \quad 995 \quad 14,866 \quad 592 \quad 1,417 \quad .95897303573732 \quad 1.00 \quad 0.00 \quad 0.288 \quad 10.27E+07 \quad 1.27E+07 \quad 1.27E+0$ 

 $\text{CR-CO-HR-08-11} \quad 39.25931 \quad 106.4771 \quad 3,682 \quad 3 \quad 2.73 \quad 1.00 \quad 0.00 \quad 0.2825 \quad 17.761 \quad 2,516.63 \quad 38.3943 \quad 4.74\text{E}+07 \quad 7.25\text{E}+05 \quad 2.67\text{E}+06 \quad 4.08\text{E}+04 \quad 07\text{KNSTD} \quad 9,566.13 \quad 321.992 \quad 3.03\text{E}+08 \quad 1.02\text{E}+07 \quad 1.71\text{E}+07 \quad 5.75\text{E}+05 \quad \text{KNSTD} \quad 6.39101208961966 \quad 47,925 \quad 741 \quad 2,956 \quad 44,834 \quad 1,541 \quad 4,233 \quad .93550339071466 \quad 4.081\text{E}+07 \quad 1.71\text{E}+07 \quad 1.71\text{$ 

 $\text{CR-CO-HR-09-11} \quad 39.26566 \quad 106.485 \quad 3,627 \quad 3 \quad 2.73 \quad 1.00 \quad 0.00 \quad 0.2775 \quad 51.627 \quad 8,389.71 \quad 103.156 \quad 1.56E+08 \quad 1.91E+06 \quad 3.01E+06 \quad 3.71E+04 \quad 0.7KNSTD \quad 21,658.7 \quad 501.35 \quad 1.01E+09 \quad 2.34E+07 \quad 1.96E+07 \quad 4.54E+05 \quad KNSTD \quad 6.5056743904202 \quad 57,784 \quad 723 \quad 3,534 \quad 55,841 \quad 1,330 \quad 5,113 \quad .96637477502423 \quad 1.96E+07 \quad 1.9$ 

 $\text{CR-CO-HR-01-15} \quad 39.36029 \quad 106.4896 \quad 3,627 \quad 3 \quad 2.73 \quad 1.00 \quad 0.00 \quad 0.2894 \quad 37.1230010986328 \quad 1,320.36 \quad 23.879 \quad 2.55E+07 \quad 4.62E+05 \quad 6.87E+05 \quad 1.21E+05 \quad KNSTD \quad 6.80696991327569 \quad 13,667 \quad 248 \quad 846 \quad 13,714 \quad 357 \quad 1,240 \quad 1.00343894051365 \quad 1.21E+05 \quad 1.21$ 

 $\text{CR-CO-HR-02-15} \quad 39.36017 \quad 106.48977 \quad 3,627 \quad 3 \\ & 2.73 \quad 1.00 \quad 0.00 \quad 0.2674 \quad 46.4869995117188 \quad 1,549.02 \quad 29.2964 \quad 2.77E+07 \quad 5.24E+05 \quad 5.95E+05 \quad 1.13E+06 \quad 1.13E+05 \quad \text{KNSTD} \quad 7.23496537773483 \quad 11,377 \quad 217 \quad 707 \quad 12,444 \quad 328 \quad 1,126 \quad 1.09378570800738 \\ & 1.126 \quad 1.09378570800738 \quad 1.09378570800738 \quad 1.09378570800738 \\ & 1.126 \quad 1.093785708$ 

 $\text{CR-CO-HR-03-15} \quad 39.36002 \quad 106.49004 \quad 3,627 \quad 3 \quad 2.73 \quad 1.00 \quad 0.00 \quad 0.2609 \quad 50.1650009155273 \quad 1,868.82 \quad 32.1205 \quad 3.26E+07 \quad 5.60E+05 \quad 4.75E+06 \quad 1.21E+05 \quad KNSTD \quad 7.31630456381456 \quad 12,862 \quad 223 \quad 793 \quad 13,961 \quad 358 \quad 1,261 \quad 1.08544549836728 \quad 1.085445498728 \quad 1.085445498728 \quad 1.085445498728 \quad 1.08$ 

 $\text{CR-CO-HR-04-15} \quad 39.36833 \quad 106.48904 \quad 3,545 \quad 3 \\ 2.73 \quad 1.00 \quad 0.00 \quad 0.264 \quad 24.7320003509521 \quad 927.879 \quad 18.3557 \quad 1.64E+05 \quad 47.1622 \quad 1.12E+08 \quad 3.65E+06 \quad 4.54E+06 \quad 1.47E+05 \quad KNSTD \quad 6.86450777697456 \quad 13,849 \quad 275 \quad 865 \quad 14,018 \quad 457 \quad 1,297 \quad 1.01220304715142 \\ 1.12E+08 \quad 1.12E$ 

 $\text{CR-CO-HR-05-15} \quad 39.36803 \quad 106.48937 \quad 3,545 \quad 3 \quad 2.73 \quad 0.99 \quad 0.00 \quad 0.261 \quad 22.1450004577637 \quad 844.829 \quad 16.8638 \quad 1.47\text{E}+07 \quad 2.94\text{E}+05 \quad 6.65\text{E}+05 \quad 1.31\text{E}+06 \quad 5.27\text{E}+06 \quad 1.61\text{E}+05 \quad KNSTD \quad 7.93620038192057 \quad 13,992 \quad 281 \quad 875 \quad 16,136 \quad 497 \quad 1,484 \quad 1.15323041738136 \quad 12.466 \quad 1.17\text{E}+08 \quad 1.27\text{E}+08 \quad 1$ 

 $\text{CR-CO-HR-08-15} \quad 39.36948 \quad 106.48501 \quad 3,450 \quad 3 \quad 2.73 \quad 0.99 \quad 0.00 \quad 0.2664 \quad 14.6569995880127 \quad 479.506 \quad 10.645 \quad 8.52E+06 \quad 1.90E+05 \quad 5.81E+05 \quad 1.29E+06 \quad 3.92E+06 \quad 3.92E+06 \quad 3.92E+06 \quad 1.50E+05 \quad KNSTD \quad 6.74133788881907 \quad 12,902 \quad 287 \quad 816 \quad 12,762 \quad 491 \quad 1,209 \quad .98914896915207 \\ \textbf{CR-CO-HR-08-15} \quad 39.36948 \quad 106.48501 \quad 3,450 \quad 3 \quad 2.73 \quad 0.99 \quad 0.00 \quad 0.2664 \quad 14.6569995880127 \quad 479.506 \quad 10.645 \quad 8.52E+06 \quad 1.90E+05 \quad 5.81E+05 \quad 1.29E+06 \quad 1.90E+05 \quad 1.9$ 

 $\text{CR-CO-HR-10-15} \quad 39.27922 \quad 106.49874 \quad 3,697 \quad 3 \\ 2.73 \quad 1.00 \quad 0.00 \quad 0.2623 \quad 50.2540016174316 \quad 10,522.5 \quad 107.537 \quad 1.84E+08 \quad 1.89E+06 \quad 3.67E+06 \quad 3.75E+04 \quad 07KNSTD \quad 12,370.2 \quad 429.755 \quad 1.25E+09 \quad 4.35E+07 \quad 2.49E+07 \quad 8.65E+05 \quad KNSTD \quad 6.78472381447243 \quad 66,271 \quad 688 \quad 4,035 \quad 66,987 \quad 2,405 \quad 6,422 \quad 1.01080412246684 \quad 1.0108041246684 \quad 1.01080$ 

 $\text{CR-CO-HR-11-15} \quad 39.27808 \quad 106.49824 \quad 3,682 \quad 3 \quad 2.73 \quad 1.00 \quad 0.00 \quad 0.2637 \quad 36.3400001525879 \quad 6,256.03 \quad 64.3355 \quad 1.10\text{E}+08 \quad 1.13\text{E}+06 \quad 3.03\text{E}+06 \quad 3.12\text{E}+04 \quad 07KNSTD \quad 31,105.4 \quad 1,073.89 \quad 7.58\text{E}+08 \quad 2.62\text{E}+07 \quad 2.09\text{E}+07 \quad 7.20\text{E}+05 \quad KNSTD \quad 6.87785705147357 \quad 56,201 \quad 587 \quad 3,414 \quad 57,737 \quad 2,047 \quad 5,504 \quad 1.02733047454672 \quad 1.027330$ 

 $\text{CR-CO-HR-12-15} \quad 39.27754 \quad 106.49722 \quad 3,676 \quad 3 \quad 2.73 \quad 1.00 \quad 0.00 \quad 0.2716 \quad 30.7369995117188 \quad 7,682.92 \quad 75.6508 \quad 1.37E+06 \quad 4.47E+04 \quad 07KNSTD \quad 27,641. \quad 695.408 \quad 9.43E+08 \quad 2.37E+07 \quad 3.07E+07 \quad 7.72E+05 \quad KNSTD \quad 6.76514594725177 \quad 83,589 \quad 840 \quad 5,106 \quad 84,599 \quad 2,218 \quad 7,904 \quad 1.01208292957207 \quad 1.0120829297207 \quad 1.0120829297207 \quad 1.0120829297207 \quad 1.0120829297207 \quad 1.0120829297207 \quad 1.0120829297207 \quad 1.012$ 

 $\text{CR-CO-HR-13-15} \quad 39.26778 \quad 106.48619 \quad 3,642 \quad 3 \quad 2.73 \quad 1.00 \quad 0.00 \quad 0.2631 \quad 48.5270004272461 \quad 3,568.01 \quad 66.9524 \quad 6.27E+07 \quad 1.18E+06 \quad 2.32E+05 \quad \text{KNSTD} \quad 6.95539762762901 \quad 24,048 \quad 456 \quad 1,498 \quad 24,662 \quad 644 \quad 2,241 \quad 1.02553226879574 \quad 2.73 \quad 1.00 \quad 0.00 \quad 0.2631 \quad 48.5270004272461 \quad 3,568.01 \quad 66.9524 \quad 6.27E+07 \quad 1.18E+06 \quad 1.29E+06 \quad 2.32E+05 \quad \text{KNSTD} \quad 6.95539762762901 \quad 24,048 \quad 456 \quad 1,498 \quad 24,662 \quad 644 \quad 2,241 \quad 1.02553226879574 \quad 2.73 \quad 1.00 \quad 0.00 \quad 0.2631 \quad 48.5270004272461 \quad 3,568.01 \quad 66.9524 \quad 6.27E+07 \quad 1.18E+06 \quad 1.29E+06 \quad 2.32E+05 \quad \text{KNSTD} \quad 6.95539762762901 \quad 24,048 \quad 456 \quad 1,498 \quad 24,662 \quad 644 \quad 2,241 \quad 1.02553226879574 \quad 2.73 \quad 1.00 \quad 0.00 \quad 0.2631 \quad 48.5270004272461 \quad 3,568.01 \quad 66.9524 \quad 6.27E+07 \quad 1.18E+06 \quad 1.29E+06 \quad 2.32E+05 \quad \text{KNSTD} \quad 6.95539762762901 \quad 24,048 \quad 456 \quad 1,498 \quad 24,662 \quad 644 \quad 2,241 \quad 1.02553226879574 \quad 2.73 \quad 1.00 \quad 0.00 \quad 0.2631 \quad 48.5270004272461 \quad 3,568.01 \quad 2.00 \quad 2.00$ 

 $\text{CR-CO-HR-14-15} \quad 39.26778 \quad 106.48619 \quad 3,642 \quad 3 \quad 2.73 \quad 1.00 \quad 0.00 \quad 0.2565 \quad 38.3089981079102 \quad 3,768.54 \quad 54.8209 \quad 6.46E+07 \quad 9.40E+05 \quad 1.69E+06 \quad 2.45E+04 \quad 07KNSTD \quad 15,479.3 \quad 471.266 \quad 4.25E+04 \quad 07KNSTD \quad 15,479.3 \quad 471.266 \quad 4.25E+04 \quad 07KNSTD \quad 15,479.3 \quad 471.266 \quad 4.25E+08 \quad 1.29E+07 \quad 1.11E+07 \quad 3.38E+05 \quad KNSTD \quad 6.57831634669232 \quad 31,026 \quad 453 \quad 1,900 \quad 30,049 \quad 929 \quad 2,782 \quad .96851028169922 \quad 1.29E+07 \quad 1.29E+0$ 

 $\text{CR-CO-HR-15-15} \quad 39.26778 \quad 106.48619 \quad 3,642 \quad 3 \\ \hline \ 2.73 \quad 1.00 \quad 0.00 \quad 0.2574 \quad 40.0620002746582 \quad 3,364.63 \quad 40.992 \quad 4.08E+05 \quad 1.44E+06 \quad 1.72E+04 \quad 07KNSTD \quad 16,038.3 \quad 409.922 \quad 4.08E+05 \quad 1.44E+06 \quad 1.72E+04 \quad 07KNSTD \quad 16,038.3 \quad 409.922 \quad 4.08E+08 \quad 1.04E+07 \quad 1.02E+07 \quad 2.61E+07 \quad 1.02E+07 \quad 1.04E+07 \quad 1.04E$ 

 $\text{CR-CO-HR-17-15} \quad 39.25788 \quad 106.48277 \quad 3,627 \quad 3 \quad 2.73 \quad 1.00 \quad 0.00 \quad 0.2617 \quad 33.0900001525879 \quad 185.448 \quad 7.35771 \quad 3.22E+06 \quad 1.29E+05 \quad 9.74E+04 \quad 3.89E+03 \quad 07KNSTD \quad 479.671 \quad 18.5894 \quad 2.58E+07 \quad 1.00E+06 \quad 7.80E+05 \quad 3.02E+04 \quad KNSTD \quad 8.0020325678532 \quad 2,174 \quad 87 \quad 155 \quad 2,534 \quad 98 \quad 239 \quad 1.16559337626495 \quad 1.29E+05 \quad 1.$ 

2.82054 .95151 ---

Rock unit patterns show generalized direction of foliation as interpreted from field measurements.

CR-CO-HR-01-11 39.33011 106.4082 3,341 3 2.73 0.99 0.00 0.2705 6.79

CR-CO-HR-02-11 39.32831 106.417 3.450 3 2.73 0.99 0.00 0.2793 7.417

CR-CO-HR-04-11 39.35044 106.4121 3,450 3 2.73 0.99 0.00 0.2728 9.922

CONVERSION FACTORS

millimeter (mm)

kilometer (km)

centimeter (cm)

International System of Units to U.S. customary units

Any use of trade, firm, or product names is for descriptive purposes only and does not imply

scale may occur when viewing it on a computer screen or when printing it on an electroni

This map is offered as an online-only, digital publication. Users should be aware that

plotter, even when it is viewed or printed at its intended publication scale.

-- -- 0.2828 --

formulated the cosmogenic chronologies reported herei

Manuscript approved for publication February 24, 2020

Edit and digital cartographic production by Lisa J. Binder, Julie A. Herrick, and Stuart A. Giles

GIS database and digital cartography by Brandt

 $(10^{-15}) \qquad (10^{-15}) \qquad (atoms) \qquad (atoms/g) \qquad (atoms/g)$ 

212.367 6.7921 3.76E+06 1.24E+05 5.53E+05 1.83E+04 07KNSTD 500.51 20.1648 2.41E+07 9.74E+05 3.55E+06 1.43E+05 KNSTD 6.41235768614353 13,195 438 896 12,204 495 1,166 .92489579386131

226.555 9.8323 4.15E+06 1.84E+05 5.59E+05 2.49E+04 07KNSTD 1,122.33 50.9018 2.78E+07 1.26E+06 3.75E+06 1.70E+05 KNSTD 6.71413386103306 12,241 547 908 11,971 546 1,171 .97794297851483

336.449 10.1348 6.05E+06 1.86E+05 6.10E+05 1.87E+04 07KNSTD 888.432 38.4499 4.01E+07 1.73E+06 4.04E+06 1.75E+05 KNSTD 6.61811204530715 13,553 417 904 13,161 574 1,276 .97107651442485

 $710.952 \qquad 17.4247 \qquad 1.34E + 07 \qquad 3.30E + 05 \qquad 6.71E + 05 \qquad 1.66E + 04 \qquad 07KNSTD \qquad 3.265.78 \qquad 103.087 \qquad 8.89E + 07 \qquad 2.81E + 06 \qquad 4.47E + 06 \qquad 1.41E + 05 \qquad KNSTD \qquad 6.65110917891957 \qquad 12,883 \qquad 320 \qquad 827 \qquad 12,543 \qquad 398 \qquad 1,156 \qquad .97360863152992 \qquad 12,543 \qquad 103.087 \qquad 12,543 \qquad$ 

222.771 8.65827 4.20E+06 1.68E+05 6.02E+05 2.40E+04 07KNSTD 601.581 26.4621 2.86E+07 1.26E+06 4.10E+06 1.80E+05 KNSTD 6.81412130859081 12,993 520 928 13,015 575 1,265 1.00169321942584

Birkeland, 1980), but mantle relict ice bodies formed during former glacial episodes. Active rock glaciers in the Front Range, north of the region, have estimated rates of movement of 1–10 centimeters per year (cm/yr) (White, 1971, 1976). Thickness 20–50 m **Qgp Outwash gravel of Pinedale glaciation (late Pleistocene)**—Pebble, cobble, and boulder gravel with a silty sand matrix interbedded with sand and sandy pebble layers and lenses underlying terraces grading to unit Qtp. Clasts are subrounded to rounded and generally <1 m in diameter. Deposit is locally clast supported with little to no matrix. Maximum deposition of unit is correlated with the LGM (Pinedale) about 22–20 ka and higher-energy glaciofluvial deposition to have waned or terminated by about 14–13 ka (this report). Pedogenic soils typically have an A/Bw/C profile. Clast composition consists of chiefly Proterozoic metamorphic rocks derived from the surrounding region. Height of terrace treads above active stream channels ranges from 3–10 m. Source is primarily reworked till of Pinedale glaciation along tributary streams. Mapped and differentiated adjacent to the Turquoise Lake inlet. Small unmapped, remnant deposits of this unit can be found along active drainages but are discontinuous and generally thin due to the erosive geomorphic environment during the LGM about 22–20 ka and its deglaciation. Thickness varies with geomorphic location within the basin, but generally ranges from 1–5 m Till of Pinedale glaciation (late Pleistocene)—Subangular to subrounded, unconsolidated, pebble- to boulder-sized clasts in a clayey, silty sand matrix. Deposits generally poorly sorted to unsorted. Clasts range up to is characterized by steep-crested lateral moraines and undrained hummocky depressions within terminal and recessional moraine

MESOPROTEROZOIO

10 m in diameter and are competent with very little weathering. Deposit complexes deposited directly by glacial ice. Locally has sorted and bedded lenses of sandy gravels deposited by subglacial streams. Convoluted and disturbed bedding due to minor glacial advances is locally preserved. Soils on deposits are generally characterized by weak to moderately developed Bw horizons, but locally have weak Bt horizons of stage I development. Clasts are chiefly unweathered and competent, except where older deposits have been reworked into deposits of Qtp. Age of deposits are constrained by Beryllium-10 (<sup>10</sup>Be) and Aluminum-26 (26Al) cosmogenic nuclide ages on exposed surface boulders that generally range from about 22–13 ka within the quadrangle (table 1). Other studies within the region indicate Pinedale glaciation to have occurred between 30–12 ka (Madole, 1986; Nelson and Shroba, 1998; Benson and others, 2004, 2005) with the LGM being about 22-20 ka and a possible ice advance or stagnation at about 15.5–14.5 ka (Brugger, 2007; Briner, 2009; Mason and others, 2011; Young and others, 2011; Ruleman and others, 2013). Complete deglaciation of the northern Sawatch Range occurred by about 14–13 ka (Ruleman and others, 2013; 2018) (see table 1). Estimated thickness is 3–60 m Till of Bull Lake glaciation (late middle Pleistocene)—Subangular to

Quaternary Deposits

Neogene Basin Fill

Arkansas Valley; AR, Arkansas River.

Neogene Volcanic Rocks, Basalt and lesser rhyolite

Paleocene and Late Cretaceous Intrusive Rocks

Paleocene to Jurassic Sedimentary Rocks

Permian to Cambrian Sedimentary Rocks

Figure 1. Geologic setting of the Homestake Reservoir, Colo., 7.5' quadrangle (modified from Ruleman and others [2018]). Black box indicates location of mapped

quadrangle. Major Laramide and older structures shown by heavy black lines. Faults having definitive Pleistocene activity shown by heavy red lines. UAV, Upper

----- Fault—Major Laramide and

Active fault—Definitive

in the vicinity of Leadville and the northern Mosquito Range (Behre,

1953; Bohannon and Ruleman, 2013; Ruleman and others, 2018), but the

age of the mapped Lincoln Porphyry remains problematic. Biotite K-Ar

ages are documented in an older and younger suite, 62 and 64.6 million

years (Ma) (respectively Pearson and others, 1962; McCalpin and others,

younger, fission- track dates of 36.7±3.9 and 48.6±6.6 Ma on apatite and

40.1±3.9 and 41.5±3.7 Ma on zircon (Mach, 1992) have been obtained

from rocks of very similar composition and appearance to the Lincoln

Porphyry mapped to the east within the Climax, Colo., 7.5' quadrangle

(McCalpin and others, 2012), although they may not be the same unit.

history of the region, we speculate that the older Paleocene ages are

measurements of xenolithic bodies and inclusions of the older White

porphyry, with ages of 71.8–64.1±0.9 Ma (Cunningham and others,

1994; Kellogg and others, 2017; Ruleman and others, 2018)

**Tkw** White porphyry group dikes (Paleocene and Upper Cretaceous)—White

to yellowish brown, fine-grained cryptocrystalline to aphanitic

Tku Unclassified porphyry dikes (Tertiary and Cretaceous)—Generally white,

of the Isolation Lake cirque basin

Based on geologic mapping by Tweto (1974) and the complex intrusive

red, yellow, and brown, highly altered and sheared porphyries of various

composition. Exposed as a northeast-trending dike on the headwall east

porphyritic rhyolite and monzogranite. Composed primarily of visible

apatite, and hornblende (Cappa and Bartos, 2007). Generally exposed

quartz and biotite <2 mm in a fine-grained groundmass of quartz, biotite,

and plagioclase. Common accessory minerals include magnetite, zircon,

across the southern half of the quadrangle in east-west-trending dikes. To

the east and southeast of the quadrangle dikes continue across the western

Formation on the Leadville South quadrangle (Ruleman and others, 2018)

thickening to the south-southeast into domed sills and small stocks in the

Mount Sherman quadrangle (Bohannon and Ruleman, 2013). Unit includes

the Pando Porphyry of Tweto (1951; 1974) dated at 70 Ma (Pearson and

others, 1962), 71.8 Ma (Cunningham and others, 1994) and a more recent

hornblende granodiorite. Intrudes biotite gneiss, impure quartzite, and

St. Kevin Granite (Ygs) with sharp contacts. Distinguished from St.

Kevin Granite by lack of muscovite. Occurs in a small stock at West

Tennessee Lakes in the north-central part of the quadrangle and within

U-Pb zircon age of 64.1±0.9 Ma (Kellogg and others, 2017)

concealed dikes along the central-eastern portion of the map

PROTEROZOIC IGNEOUS AND METAMORPHIC ROCKS

MESOPROTEROZOIC SHEAR ZONE ROCKS

Mylonite series shear zone rocks and pseudotachylite (Mesoproterozoic)-

shear zones. Textures show evidence for grain-size reduction,

Mylonite-series rocks consist of fine-grained, strongly foliated and

porphyroblast and porphyroclast rotation, and mineral elongation in

plastically sheared rock (Shaw and others, 2001; Lee and others, 2012).

Hosted by biotite gneiss (Xb), hornblende gneiss (Xhch), and impure

others, 2012). Locally overprinted by pseudotachylite and mylonitic

quartzite (Xhcq). Mylonitic foliations typically trend subparallel to host-

rock foliations, although they locally crosscut the older fabric (Lee and

pseudotachylite. Exposed in the Slide Lake shear zone in the northeastern

Reservoir quadrangle in the Homestake shear zone. Electron microprobe

uranium-thorium-lead (U-Th-Pb) monazite dating from the Homestake

(Shaw and others, 2001). Pseudotachylite consists of black to dark gray

shear zone suggests deformation ca. 1.42–1.38 billion years ago (Ga)

veins of amorphous fault rock <1 cm thick. Locally mylonitized and

oblique angle to the fault plane. Contains rapidly quenched

recrystallized to fine-grained biotite (Merson and others, 2015). Occurs

as foliation-parallel veins filling brittle faults, and as injection veins at an

disequilibrium melt and clasts of wall rock formed during brittle, high

temperature, and high strain rate seismic slip (Allen and others, 2002).

Hosted by biotite gneiss, impure quartzite, and St. Kevin Granite. Occurs

in association with ultramylonite on ridge northeast of Homestake Peak

Homestake Reservoir, and north of the Homestake Reservoir quadrangle

coarse-grained to megacrystic, white to light-pink and red, inequigranular

"chilled," aplitic textures formed towards the margins. Pegmatites within

quartz-feldspar-biotite-muscovite rock. Biotite is the main mica. Forms

tourmaline and beryl (Tweto, 1974). Pegmatite and aplite are similar in

composition, but aplite is generally light pinkish brown to gray, fine to

medium grained, and leucocratic, which can be similar in appearance to

undivided (Mesoproterozoic and Paleoproterozoic)—Medium-gray to

zoned, linear dikes and irregular intrusions typically with fine-grained

and proximal to the St. Kevin batholith locally include sparse black

the Mesoproterozoic St. Kevin Granite (Ygs), and especially the

finer-grained, marginal phases of Ygs. The unit does not show

Monzogranite, granodiorite, biotite gneiss and schist, and pegmatite,

mesoscopic evidence for solid-state plastic deformation

(Shaw and others, 2001; Lee and others, 2012; Allen and Shaw, 2013).

Exposed in the Slide Lake shear zone, St. Kevin Granite east of

MESOPROTEROZOIC AND PALEOPROTEROZOIC IGNEOUS

AND METAMORPHIC ROCKS

in the Homestake shear zone (Allen, 2005; Shaw and Allen, 2007)

Pegmatite and aplite (Mesoproterozoic and Paleoproterozoic)—Fine- to

corner of the quadrangle (Frothingham, 2017), and north of the Homestake

lineated rock including mylonite and ultramylonite occurring in discrete

Granodiorite (Late Cretaceous)—Fine- to medium-grained, gray biotite-

flank of Mount Zion as sills subparallel to bedding within the Minturn

2012), and  $44.1\pm1.6$  Ma (Marvin and others, 1989). Supporting

subrounded, unconsolidated, unsorted and lacking bedding and stratification, pebble to boulder gravel in a clay, silt, and sand matrix. Deposits generally lie downvalley from Pinedale terminal moraines (unit Qtp). The original depositional surface morphology has been eroded and smoothed. Boulders are partially to mostly buried on the surface and clasts are more weathered than that of unit Qtp. Boulders in unit Qtb commonly have oxidized weathering rinds 3–5 mm in thickness and are readily friable. In this northern region of the upper Arkansas Valley, soils on these deposits are generally A/Bt/C profiles with a 20–30 cm-thick argillic horizon oxidized to slightly red chromas. To the south of the quadrangle, soils on deposits of this age commonly have stage II pedogenic carbonate development, but within the mapped quadrangle Qtb deposits typically have stage I carbonate development and locally discontinuous stage II pedogenic carbonate. Deposits are correlated with those dated in the adjacent Front Range of Colorado with <sup>10</sup>Be and <sup>26</sup>Al cosmogenic radionuclide exposure minimum age estimates of 101±21 and 122±26 ka (Schildgen and others, 2002). Thickness varies based on geomorphic position, but is generally estimated to be 5–20 m PLIOCENE? TO LATE CRETACEOUS INTRUSIVE ROCKS

**Rhyolite (Pliocene? or Miocene?)**—Fine-grained, white rhyolite and lightgray to black flow-banded vitrophyre. Occurs in north-trending dike system on eastern flank of Sawatch Range, from south edge of quadrangle to north side of Longs Gulch, and in scattered small dikes elsewhere. This rhyolite and a rhyolite breccia, occurring to the east within the Leadville North, Colo., 7.5' quadrangle (Ruleman and others, 2018), are the youngest intrusive rocks recognized in the quadrangle. Tweto (1974) inferred an age as young as Pliocene or late Miocene based on evidence of hypabyssal intrusion indicated by extensive development Latite breccia (Oligocene)—Highly altered latite and quartz latite porphyry containing brecciated Proterozoic host-rock fragments. Unit occurs in a

Divisions of Quaternary, Neogene, and Paleogene time

ressed in yr for years, ka for kilo-annum (thousand years) and Ma for

**Photograph 3.** This photograph of U.S. Geological Survey student interns Candice

of the Central Colorado Icefield during the Last Glacial Maximum ~22,000 to 20,000

years ago (Leonard and others, 2017). Photograph by C.A. Ruleman, 2015.

Passehl and Michael Frothingham displays a cosmogenic nuclide surface exposure site

on glacially scoured Proterozoic metamorphic rocks along Homestake Creek. View is

looking south towards Homestake Reservoir, with the dam just below the skyline in the

center of the photograph. This site was occupied and eroded by the Homestake glacier

Age

0-11,477±85 yr

early 788 ka-2.588 Ma

11.5–132 ka

132–788 ka

2.588-5.332 Ma

5.332-23.03 N

23.03-33.9 Ma

33.9-55.8 Ma

55.8-65.5 Ma

65.5-145 M

1,000-1,600 Ma

1,600-2,500 Ma

**Photograph 1.** View looking north from the south col

above Lake Esther in the northwest corner of the

taken from the outcrop in the immediate foreground

episodes, overrode this saddle, and many others, as

one larger ice field: the middle Pleistocene Central

olorado Icefield (Ruleman and Hudson, 2016;

ıleman and others, 2018, 2019a, 2019b).

tograph by C.A. Ruleman, 2015.

quadrangle. Cosmogenic nuclide samples were

evious middle-to-late Pleistocene glacial

Epoch

Miocene

used in this report<sup>1</sup>

Period or

Neogene

Paleogene

Mesoproterozoic

Paleoproterozoic

mega-annum (million years).

MOUNT MOUNT OF THE PANDO

NAST HOMESTAKE LEADVILLE

SIM 3451

MOUNT | MOUNT | LEADVILLE

CHAMPION MASSIVE SOUTH

Index map showing map area in yellow, and adjacent

publication number, author(s), and year of publication

U.S. Geological Survey 7.5' quadrangles with the

JACKSON HOLY CROSS

single, small body within units Xb, YXmr, and Ygs south of Timberline Lake in the southwest part of the quadrangle. Originally mapped by Lincoln Porphyry (Eocene)—Light gray to light bluish-gray and pinkishgray quartz monzogranite porphyry. Contains phenocrysts of mainly orthoclase and quartz <1 cm long, and rare biotite and hornblende. Occurs in a single, small body within St. Kevin batholith north of Turquoise Lake (Tweto, 1974). Exposed as a main sill body on Cooper Hill and the western flank of Buckeye Peak and Chicago Ridge in northeastern part of the Leadville North, Colo., 7.5' quadrangle (Ruleman and others, 2018). Unit is crosscut by the gray porphyry group (Tg of Ruleman and others, 2018), mapped to the east of the quadrangle

black, grayish-pink, light-pinkish-brown to light-brown, fine- to coarsegrained biotite gneiss and schist profusely intruded by Ygs and YXp. Mineralogy is generally consistent with the parent rock and younger intrusive complexes consisting of biotite, hornblende, plagioclase, microcline, and quartz. Unit is mapped around the peripheries of the St. Kevin batholith and associated stocks and other textural or gradational phases where the intrusive component and country rock are in relatively equal proportions. Contacts commonly correspond to Tweto (1974) migmatite unit excluding older in situ migmatitic biotite gneiss. Exposures show complicated intrusive relationships and assimilation of country rock consisting predominantly of unit Xb in this region. Ptygmatic folding, boudinage, and sigmoidal structures are common. Xenolithic bodies have diffuse boundaries and locally internal, intense ptygmatic folding. Unit was mapped in regions adjacent to the St. Kevin Granite that are pervasively intruded by granite and pegmatite to distinguish this intrusive complex from areas of migmatite with evidence for in situ melting (for example, biotite selvages around granitic leucosomes) of metamorphic and meta-igneous rocks (Ruleman and others, 2011; Bohannon and Ruleman, 2013; Kellogg and others, 2017) YXdd | Diorite dikes (Mesoproterozoic and Paleoproterozoic)—Scattered dioritic dikes of various mineralogic compositions and ages. Some probably as

old as granite of Cross Creek, and some are younger than St. Kevin

Granite (Tweto, 1974) Hornblende diorite (Mesoproterozoic)—Gray, dark gray, to green, mediumgrained hornblende-rich diorite. Distinguishable from metalamprophyres (Yml) by lighter color and lack of strong foliations or lineations. Truncates Paleoproterozoic host rock foliations. Hosts metalamprophyres and St. Kevin Granite in places. Occurs in elongate pod on the East Fork of Homestake Creek and in scattered dikes near Homestake Reservoir, Upper Homestake Lake, and Slide Lake. Occurs in dikes throughout the region (Tweto, 1974). Dashed where rafted in St. Kevin Granite. Solid line where in situ as original intrusion, dashed line where hosted as pendants in younger St. Kevin Granite and mixed rock

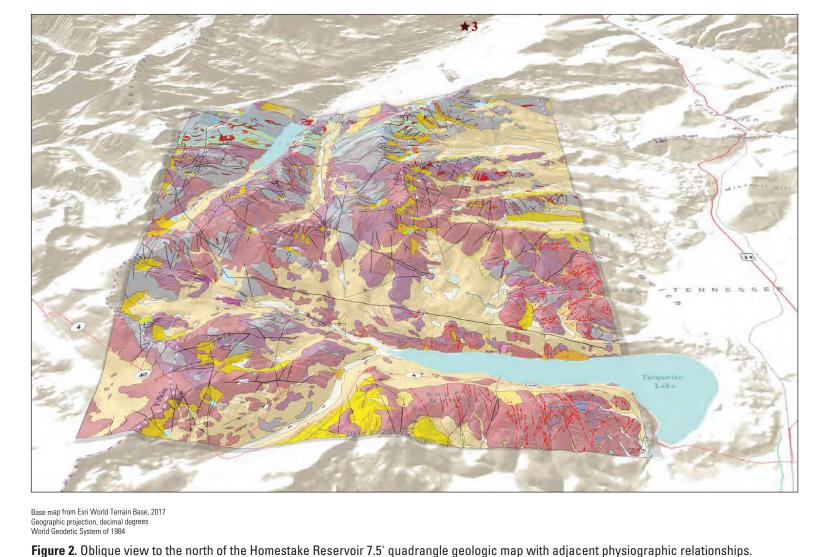
**E. Kevin Granite (Mesoproterozoic)**—Medium- to coarse-grained, gray to light-pinkish-gray and pinkish-brown, euhedral equigranular to porphyritic, massive to locally weakly foliated biotite-muscovite monzogranite, with local gradational changes to granodiorite and other textural variations (Pearson and others, 1962; Tweto and Pearson, 1964; Tweto, 1974, 1987). The main batholith is characterized by a central region of coarse-grained monzogranite grading outward into mediumgrained monzogranite and fine-grained foliated monzogranite and granodiorite with seriate-to-porphyritic texture commonly having Carlsbad twinning in aligned microcline phenocrysts. Within the map area, medium-grained, euhedral monzogranite is the common phase of the main plutonic body. Silicified, quartz-rich zones are mapped along the central-eastern portion of the map (Tweto, 1974) and indicated by dark blue, solid lines within unit Ygs. Rb-Sr isochron age is 1,390±60 Ma (Pearson and others, 1962), and a more recent U-Pb age from outside the quadrangle is 1,442±14 Ma (Moscati and others, 2017). Hydrothermally altered St. Kevin Granite, unit Ygs(a), bounds the north and south sides of the central region of Turquoise Lake along a generally north-trending fault zone. Farther north along the same north-trending fault zone, sheared and brecciated St. Kevin Granite, Ygs(s), is mapped between Porcupine and Longs Gulches and along the ridge between Homestake Reservoir and East Fork Homestake Creek

etalamprophyre (Mesoproterozoic)—Dark gray, brown to gray green, mafic, ultrapotassic, foliated and lineated, porphyritic dikes (Yml dikes). Matrix modal mineralogy includes on average 35 percent biotite, 30 percent potassium feldspar, 20 percent quartz, and 15 percent hornblende (Frothingham, 2017). Porphyroblast modal mineralogy includes on average 60 percent hornblende and 40 percent biotite. Metalamprophyres display strong foliations near their margins, and moderate foliations near the center of the dikes. Foliations are defined by compositional banding of feldspar and quartz in felsic lenses, and biotite and hornblende in mafic lenses. Strong grain shape preferred orientations in biotite, and moderate grain shape preferred orientations in hornblende also contribute to foliations. Lineations, when present, are defined by elongated porphyroblasts of hornblende and biotite. Porphyroblasts are mostly undeformed near dike centers and are strongly elongated near dike margins. Occur in highest concentrations in the northern half of the quadrangle and northwestern quadrant as east northeast-trending, subvertical dikes, approximately following preexisting foliations in Paleoproterozoic biotite gneiss. Metalamprophyres are also found in lesser concentrations in the southern half of the quadrangle as discontinuous pendants hosted by the younger, intrusive St. Kevin batholith. Whole rock x-ray fluorescence (XRF) geochemical analyses by Barbery and others (2013) suggest that metalamprophyres were emplaced as calc-alkaline lamprophyres to lamproitic lamprophyres, based on classification by Rock (1987). Metalamprophyres were metamorphosed and deformed broadly contemporaneous to deformation in the adjacent Homestake shear zone ca. 1,420–1,380 Ma (Shaw and others, 2001) nclassified granite (Paleoproterozoic)—Pink to gray, medium-grained, quigranular, biotite granite. Other minerals include quartz, plagioclase,

muscovite. Intruded by metalamprophyres (Yml). Occurs in small body west of Homestake Reservoir along the contact between biotite gneiss (Xb) and hornblende gneiss (Xhch) Xdi Biotite-quartz diorite dikes (Paleoproterozoic)—Gray to dark-gray mediumto coarse-grained moderately to strongly foliated diorite. Limited to the southwest quadrant of the map as two north- and one northeast-trending dikes. Inferred to be related to granite of Cross Creek (Tweto, 1974) Biotite gneiss (Paleoproterozoic)—Gray to brown, foliated, biotite-rich

and microcline. Distinguished from St. Kevin batholith by lack of

quartzofeldspathic gneiss, locally migmatitic. Modal mineralogy includes on average 55 percent quartz, 20 percent biotite, 10 percent muscovite, 5 percent sillimanite, 5 percent potassium-feldspar, and 5 percent opaques (Frothingham, 2017). Locally contains garnets as much as 1 cm in diameter. Foliations are defined primarily by compositional banding of quartz-rich leucosomes and biotite-rich melanosomes. Felsic leucosomes are on average between 1–10 mm thick, but may be as thick as 1 m. Melanosomes, primarily consisting of aligned biotite selvages, vary from less than 1 mm to more than 10 cm thick. Foliations are straight in high-strain lenses and are structurally chaotic and disorganized in low-strain lenses. Biotite gneiss occurs as the primary basement rock in the northern half of the quadrangle, and as large (>1 kilometer [km]) pendants within the St. Kevin batholith in the southern half of the quadrangle. Biotite gneiss is highly interfingered with other units such as



The location of photograph 3 is marked by star. hornblende gneiss, impure quartzite, and impure marble in the northern

half of the quadrangle. Biotite gneiss is interpreted to be part of a metasedimentary to metavolcanic supracrustal succession (Tweto, 1987; Allen and Shaw, 2013), originally deposited ca. 1,785–1,770 Ma (Wallace, 1993), and metamorphosed in the amphibolite facies ca. 1.71–1.63 Ga (Shaw and others, 2001). Correlated with similar metasedimentary rocks within the adjacent Gore and Front Ranges with detrital zircon U-Pb ages ranging from about 1,785–1,750 Ma (Kellogg and others, 2008, 2011) **Hornblende gneiss (Paleoproterozoic)**—Gray to dark gray, weakly foliated, and locally sheared hornblende and plagioclase-rich gneiss (Frothingham,

2017). Modal mineralogy includes on average 60 percent hornblende, 30 percent plagioclase, 5 percent biotite, 5 percent chlorite, and trace opaques. Minor quartz and microcline may also occur when adjacent to other quartzofeldspathic gneiss. Foliations are defined by moderate to strong compositional banding. Weak grain shape preferred orientations also contribute to foliations. Hornblende-rich melanosomes vary from 1 to 100 mm thick. Foliations are straight in high-strain lenses and are structurally chaotic and disorganized in low-strain lenses. Hornblende gneiss occurs primarily in the northern half of the quadrangle as part of an about 2-km-wide, east-to-west-trending band of highly interfingered biotite gneiss, impure quartzite, and impure marble. Hornblende gneiss is interpreted to be metavolcanic in origin (Tweto, 1987). A prominent east-west-trending shear zone, Xhch(s), lies within unit along the north side of Paradise Lakes

Xhcm Impure marble (Paleoproterozoic)—White, light to medium gray, to bluishgreen, weakly foliated calc-silicate gneiss to a nearly pure marble (Frothingham, 2017). Modal mineralogy on average includes 45 percent clinopyroxene, 40 percent calcite, and 15 percent microcline. Other minerals include biotite, quartz, feldspar, hornblende, orthopyroxene, and chlorite. Foliations are rarely observed on the outcrop scale or thin section scale, unless mixed with other hornblende gneiss or quartzofeldspathic gneiss. Impure marble displays hackly weathering in outcrop and reacts to dilute hydrochloric acid. Impure marble occurs primarily in the northern half of the quadrangle in part of a 2-km-wide, east-to-westtrending band of highly interfingered biotite gneiss, hornblende gneiss, and impure quartzite. Individual marble lenses are rarely more than 1 m thick. Impure marble is interpreted to be metasedimentary in origin (Tweto, 1987)

Xhcq Impure quartzite (Paleoproterozoic)—Light gray to gray green, weakly foliated, nearly pure quartzite, to a moderately gray, biotite-bearing, quartzofeldspathic gneiss (Frothingham, 2017). Most occurrences have average modal mineralogy of 45 percent quartz, 30 percent potassium feldspar, 20 percent biotite, and 5 percent sericite. Rare occurrences have modal mineralogy of nearly 100 percent quartz. Weak foliations are defined by moderate grain shape preferred orientation of biotite. Biotite foliation bands are generally less than 1 mm thick. Relatively pure quartzite lenses may be up to 10 m thick. Impure quartzite occurs primarily in the northern half of the quadrangle in part of a 2-km-wide, east-to-west-trending band of highly interfingered biotite gneiss, hornblende gneiss, and impure marble. Most common lithology of undivided unit Xhc of Kellogg and others (2017). Impure quartzite is interpreted to be metasedimentary in origin (Tweto, 1987)

- **Contact**—Long dashed where approximately located, short dashed where inferred. Short dashed contact lines projected above surface in cross

Fault—Long dashed where approximately located, short dashed where inferred, dotted where concealed. Question mark where identity or existence questionable. Fault attitude tick shows dip. Arrows show direction of movement (on cross section only) Normal fault—Dotted where concealed. Ball and bar on downthrown block

section indicate hypothetical orientation

Fluvial terrace scarp—Hachures point down scarp

Landslide scarp—Hachures point up scarp •••• Crest line of moraine—Sense of symmetry unspecified **————— Lineament**—Of probable and suspect tectonic origin Silicified zone—Silicified quartz-rich zones within the St. Kevin Granite

**Mylonite zone**—Mylonite-series rocks consist of fine-grained, strongly foliated and lineated rock including mylonite and ultramylonite occurring in discrete shear zones. Hosted by St. Kevin Granite Ygs(s), and hornblende gneiss Xhch(s). S indicates sheared. **Vein**—Dashed where approximately located, dotted where concealed. Vein attitude tick showing dip. Slickenline arrow showing grooves or striations on vein surface, showing bearing and plunge. Veins in central and western parts of map chiefly pyritic quartz-sulfide in

composition and silver bearing. **Inferred Pinedale glacial maximum**—On cross section only **Foliation trend**—Trend of foliation as interpreted from field measurements.

PLANAR POINT FEATURES **Inclined foliation**—Showing bearing and plunge. Inclined lineation arrow showing bearing and plunge

Vertical foliation—Showing strike Vertical lineation **←→ Horizontal lineation**—Showing strike **Inclined porphyry dike attitude**—Showing dip. Only appears in unit To **Inclined metalamprophyre dike attitude**—Showing dip. Only appears

Prospect pit or shallow shaft **Shaft**—Showing rock unit label and depth to formation observed in shaft in feet where available **Tunnel**—Long line points in direction of tunnel entrace at surface **Caved tunnel**—Long line points in direction of tunnel entrace at surface

**Sample location**—Showing sample location and identifier for <sup>10</sup>Be and

<sup>26</sup>Al cosmogenic radionuclide sample data and age analyses in kilo-annum (ka). See table 1 **★1** Location of photograph and number

AREAL FEATURE Shoreline—Showing open water

**GEOLOGIC SETTING** The Homestake Reservoir 7.5' quadrangle lies at the northern end of the Upper Arkansas Valley, where the Continental Divide at Tennessee Pass creates a low drainage divide between the Colorado and Arkansas River watersheds. The entire geology of the region has been mapped at various scales from adit to broad regional syntheses by many workers (Behr, 1935; Pearson and others, 1962; Stark and Barnes, 1935; and Epis and Chapin, 1975). All these structural and stratigraphic relationships were ultimately combined into a four 7.5' quadrangle compilation by Tweto (1974). Within our new map, we update much of the legacy nomenclature and remaining interpretations, which inherently refines the differentiation of geologic units, placement of contacts and structures, and the resulting geologic interpretations. Specifically, we have reinterpreted the previously mapped Proterozoic units of Tweto (1974) and the relationships with the surrounding country rock. This results in the preservation of many of Tweto's (1974) metasedimentary contact locations, but reinterpretation of the relationships between intrusive units, structures, and the resulting geologic interpretations. Ages of geologic units have been updated and many of the structures have been placed within a contemporary Neogene extensional tectono-magmatic framework. This update illuminates and permits improved distinction of older inactive and potentially active seismogenic structures within the map area and extends to adjacent regions. The cross section has been constructed to show relationships between Proterozoic and Neogene structures. The general geology of the quadrangle consists of metasedimentary Paleoproterozoic rocks, intruded by the Mesoproterozoic St. Kevin batholith and later Cretaceous and Tertiary intrusive complexes, and affected by multiple phases of tectonic deformation from Paleoproterozoic lithospheric assembly and stabilization, through Mesoproterozoic intracontinental tectonism, to Ancestral Rockies uplift and basin development, and culminating in Laramide mountain building and active Neogene extension. The current neotectonic extensional framework has resulted in the Arkansas River valley graben bound by the uplifted footwalls of the Sawatch and Mosquito Ranges on the west and east, respectively. Subsequent Pleistocene glacial erosion has resulted in spectacular deeply incised canyons and excellent exposures of bedrock. North-south-trending, surficial lineaments are mapped along the eastern

The Paleoproterozoic rocks within the quadrangle include biotite gneiss (Xb), hornblende gneiss (Xhch), impure quartzite (Xhcq), impure marble (Xhcm), and an unclassified granite (unit Xg). Metasedimentary rocks in the area are thought to have been originally deposited as marine sediments interlayered with mafic and felsic igneous rocks within a complex of back-arc basins and island arcs outboard of the southern margin of the Archean Wyoming Province beginning ca. 1,780 Ma (Boardman and Condie, 1986; Aleinikoff and others, 1993; Reed and others, 1993; Chamberlain, 1998; Premo and others, 2007). The northernmost of these terranes was subsequently accreted to the Wyoming province along the Cheyenne belt suture (Karlstrom and others, 1981; Duebendorfer and Houston, 1987; Houston and others, 1989; ) during the Medicine Bow orogeny between 1,780–1,740 Ma (Chamberlain, 1998). This major continental structure divides the Archean core of Laurentia from the accreted Proterozoic provinces to the south (Morozova and others, 2002; Tyson and others, 2002). Continued convergence led to the progressive southward growth of the continental lithosphere to form the Colorado Province (Bickford and others, 1986), often considered to be the northeastern extension of the Yavapai Province (Silver, 1965, 1967, 1969; Karlstrom and Bowring, 1988; Holm and others, 1998; Whitmeyer and Karlstrom, 2007). Axial planar foliations in isoclinal upright and recumbent folds record continued north-south crustal shortening between 1,710–1,630 Ma (Shaw and others, 2001) associated with deformation during the Yavapai and Mazatzal orogenic events (Karlstrom and Bowring, 1988).

margin of the quadrangle as probable strands of the Northern Sawatch fault zone

(Kellogg and others, 2017; Ruleman and others, 2017).

Mesoproterozoic intracontinental magmatism and shear zone deformation followed Paleoproterozoic accretion and deformation. Igneous units include hornblende diorite (Yhd); metalamprophyre dikes (Yml); as well as the St. Kevin Granite (Ygs), which was emplaced ca. 1,442±14 Ma (Moscati and others, 2017). The St. Kevin displays similar mineralogy and texture to other Mesoproterozoic granitoids emplaced during widespread regional magmatism throughout the southwestern United States ca. 1,400 Ma (Silver and others, 1977; Anderson and Bender, 1989; Frost and

The margins of the St. Kevin batholith are characterized by complex

interfingering of granite with the metamorphic country rock. These areas have been

mapped as mixed rock (unit YXmr) as a means to honor the complexity of the contacts at the scale of this map. We interpret these areas to include country rock of unit Xb and other Proterozoic gneiss profusely intruded by and partially assimilated into stocks and plutons of the St. Kevin Granite. These rocks were originally mapped as migmatite by Tweto (1974); however, we have chosen to designate them as mixed rock to distinguish them from in situ migmatite of probably Paleoproterozoic age that is abundant north of the quadrangle. Field relations display Mesoproterozoic igneous units intruding into preexisting metamorphic units, instead of locally derived partial melting and migmitization of Paleoproterozoic gneiss. Dikes, pods, and small bodies of pegmatite and aplite (YXp) are interpreted to represent both Paleoproterozoic and Mesoproterozoic intrusions that locally crosscut or are deformed by tectonic fabrics. The quadrangle lies immediately south of the Homestake shear zone, a major northeast-trending Mesoproterozoic structure (Shaw and others, 2001) within the Colorado mineral belt (Tweto and Sims, 1963; McCoy and others, 2005). An east-west-trending, subvertical pseudotachylyte-filled fault associated with the Homestake shear zone occurs on the ridge between Homestake Reservoir and the East Fork of Homestake Creek. Mylonite, ultramylonite, and mylonitic pseudotachylyte of the shallow to moderately dipping Slide Lake shear zone (Lee and others, 2012) are mapped in the northeastern corner of the quadrangle. Shear zones are hosted in Paleoproterozoic country rock as well as Mesoproterozoic igneous rocks. The earliest shear deformation is recorded in metalamprophyre dikes, prior to the intrusion of the St. Kevin batholith (Frothingham, 2017). The presence of mylonitic pseudotachylyte in the shear zones indicates they were seismically active during Mesoproterozoic time

at a depth sufficient for temperatures to exceed 300 °Celsius (°C) (Allen and Shaw,

With the onset of the Paleozoic era, shallow seas extended across this region (Myrow and others, 2003). Although pre-Quaternary sedimentary strata have been erosionally removed from the Homestake Reservoir quadrangle, the adjacent Leadville North 7.5' quadrangle preserves a record of Paleozoic sedimentation and tectonics in central Colorado. In the Leadville North quadrangle, the transgressive Late Cambrian Sawatch Formation is the oldest Paleozoic stratigraphic unit and was nonconformably deposited on Mesoproterozoic and Paleoproterozoic igneous and metamorphic rocks. The Sawatch Formation is overlain by a thin succession of Ordovician through Mississippian cratonic strata that record subtle early Paleozoic reactivation of the Homestake shear zone along the east-dipping limb of the Sawatch anticlinorium northeast of the Homestake Reservoir quadrangle (Allen, 2004). During the Middle Pennsylvanian, the Ancestral Rockies orogeny began (De Voto, 1980), uplifting Proterozoic basement rock east of the Homestake Reservoir quadrangle, which is recorded by deposition of the post-tectonic, regressive, coarse clastic Minturn Formation in the adjacent Leadville North quadrangle (Ruleman and others, 2018).

Following the Ancestral Rockies event, the region underwent a long interval of erosion and lowering of the topography and was subsequently inundated by the Late Jurassic-Cretaceous Western Interior Seaway. During the Late Cretaceous to Paleocene Laramide orogeny, contractional deformation formed the broad Sawatch anticlinorium. The informal White porphyry group (71.8–64.1 Ma; Tweto, 1974; Bohannon and 71.8–64.1±0.9 Ma (Cunningham and others, 1994; Kellogg and others, 2017), were emplaced during this time. The eastern limb of the Sawatch anticlinorium is preserved to the east of the quadrangle along the Mosquito Range and Mount Zion region north of

Igneous activity continued from the Paleocene into the Eocene from 62–40 Ma (Pearson and others, 1962; Kellogg and others, 2017). Within the quadrangle, about 40 Ma intrusive units are represented by the Lincoln Porphyry (Tl), a unit which has been mapped in adjacent areas using several local geographic names but have no substantial compositional distinction from one another (Bohannon and Ruleman, 2013; Ruleman and others, 2018). Based on the minimal presence of this intrusive rock within the quadrangle and its abundance in the adjacent Leadville North quadrangle, we interpret the location of the TI body on the eastern margin of the quadrangle to represent the western margin of a main intrusive complex underlying the Leadville region. As the Laramide orogeny and igneous activity waned in the Eocene (Tweto, 1975), broad erosional surfaces began to form across central Colorado and the Southern Rocky Mountains (Epis and Chapin, 1975). Remnants of these broad erosional surfaces are not found within the quadrangle, but these relict surfaces are preserved farther south along the southern end of the Mosquito Range and to the east in South Park and in the Front Range (Epis and Chapin, 1975; Chapin and Cather, 1983; Chapin and Kelley, 1997; Kirkham, 2006; Ruleman and others, 2011; Houck and others, 2012; Kirkham and others, 2012). Following the late Eocene erosional interval, regionally extensive Oligocene volcanism began, generally with inception of the Rio Grande rift and associated extensional deformation (Tweto, 1979; McCalpin and others, 2012). This deformation is represented in the quadrangle by normal faulting, uplift, and exhumation of the Paleoproterozoic and Mesoproterozoic core of the Sawatch anticlinorium. Oligocene volcanic rocks (unit Tlb) have very limited exposure within the quadrangle, but extensive exposures within quadrangles to the east (McCalpin and others, 2012; Bohannon and Ruleman, 2013; Ruleman and others, 2018) indicate a probable much larger buried pluton

The western margin of the upper Arkansas Valley graben is bound by the east-dipping northern Sawatch fault zone (NSFZ), expressed as lineaments along the eastern margin of the quadrangle. Discontinuous lineaments and linear bedrock escarpments occur along the trace of the NSFZ west of Tennessee Pass (Ruleman and others, 2017), but no conclusive displacement of late Pleistocene, or Last Glacial Maximum (LGM) (about 22–20 ka), or younger deposits or other features were identified on the quadrangle. However, relict bedrock escarpments, lineaments, and topographic depressions suggestive of Quaternary displacement are present and generally trend north-northwest to the

or stock along the eastern half of the quadrangle.

northwest of the quadrangle.

for production rates are made.

During the Pleistocene, multiple glacial cycles eroded and exhumed the older geology. Within the quadrangle, glacial deposits associated with Marine Oxygen Isotope stages (MIS) 2 (about 30–14 ka) and 6 (about 191–130 ka) (Lisiecki and Raymo, 2005) are identified; the Pinedale- and Bull Lake-equivalents, respectively. New cosmogenic ages presented herein are generally consistent with ages of other LGM (about 22–20 ka) and deglaciation (about 14–13 ka) deposits in the region (Young and others, 2011). Madole (1986) defines the LGM to have existed between 30–12 ka. <sup>10</sup>Be and <sup>26</sup>Al cosmogenic radionuclide analyses indicate that most of the quadrangle was underneath MIS 6 (that is, Bull Lake age) glacial ice. LGM terminal moraine complexes generally yield ages of about 22–20 ka with complete deglaciation by about 14–13 ka. Cols and benches that were covered and eroded by MIS 6 ice (that is, Bull Lake age), but were above the LGM ice generally yield ages ranging from 80–60 ka. Following deglaciation of the LGM, several minor cut-and-fill intervals persisted through the Holocene leaving the present geomorphic relationships and physiography. Sampling was carried out following established procedures outlined in Gosse and Phillips (2001). This included recording elevation, latitude, longitude, and topographic shielding data for each sample location, which accounts for any hindrance to <sup>10</sup>Be production from the surrounding skyline (table 1). Ages of samples were calculated using the CRONUS-Earth online calculator ver. 2.2, (University of Washington, 2019) following the time-invariant scaling model of Lal (1991) and Stone (2000). Uncertainties are reported at the 1 sigma ( $\sigma$ ) level (about 9 percent external uncertainty; Balco and others, 2008). Consistent with past studies within the region, no corrections for erosion or snow cover were applied, which allows for comparison with previous <sup>10</sup>Be chronologies reported for the upper Arkansas River valley and central Colorado (Guido and others,

2007; Briner, 2009; Ward and others, 2009; Young and others, 2011) when adjustments

Aleinikoff, J.N., Reed, J.C., Jr., and Wooden, J.L., 1993, Lead isotopic evidence for the origin of Paleo- and Mesoproterozoic rocks of the Colorado Province, U.S.A.: Precambrian Research, v. 63, no. 1–2, p. 97–122. [Also available at https://doi.org/10.1016/0301-9268(93)90007-O.] Allen, J.L., 2004, Timing, style, and significance of Cambrian through Laramide brittle Rocky Mountain Geology, v. 39, no. 2, p. 65–84. [Also available at https://doi.org/10.2113/39.2.65.]

Allen, J.L., 2005, A multi-kilometer pseudotachylyte system as an exhumed record of earthquake rupture geometry at hypocentral depths (Colorado, USA): Tectonophysics, v. 402, no. 1–4, p. 37–54. [Also available at https://doi.org/10.1016/j.tecto.2004.10.017.] Allen, J.L., O'Hara, K.D., and Moecher, D.P., 2002, Structural geometry and thermal history of pseudotachylyte from the Homestake shear zone, Sawatch Range, Colorado, in Lageson, D., ed., Science at the highest level: Geological Society of

America Field Guide, v. 3, p. 17–32. [Also available at https://doi.org/10.1130/0-8137-0003-5.17.] Allen, J.L., and Shaw, C.A., 2013, Seismogenic fault-zone processes and heterogeneity recorded by pseudotachylyte—New insights from the Homestake shear zone, Colorado, *in* Abbott, L.D., and Hancock, G.S., eds., Classic concepts and new directions, exploring 125 years of GSA discoveries in the Rocky Mountain region: Geological Society of America Field Guide, v. 33, p. 165–184. [Also available at https://doi.org/10.1130/2013.0033(05).]

Anderson, J.L., and Bender, E.E., 1989, Nature and origin of Proterozoic A-type granitic magmatism in the southwestern United States of America: Lithos, v. 23, no. 1–2, p. 19–52. [Also available at https://doi.org/10.1016/0024-4937(89)90021-2.] Balco, G., Stone, J.O., Lifton, N.A., and Dunai, T.I., 2008, A complete and easily accessible means of calculating surface exposure ages or erosion rates from <sup>10</sup>Be and <sup>26</sup>Al measurements: Quaternary Geochronology, v. 3, p. 174–195. [Also available at https://doi.org/10.1016/j.quageo.2007.12.001.]

Barbery, A., Facemyer, C., Allen, J.L., and Kuehn, S.C., 2013, Petrography and geochemistry of mafic-intermediate dikes from the northern Sawatch Range, Colorado [abs.]: Geological Society of America Abstracts with Programs, v. 45, no. 7, 583 p. [Also available at https://gsa.confex.com/gsa/2013AM/webprogram/Paper225389.html.] Behre, C.H., Jr., 1953, Geology and ore deposits of the west slope of the Mosquito Range: U.S. Geological Survey Professional Paper 235, 175 p., scale 1:12,000.

[Report also available at https://pubs.er.usgs.gov/publication/pp235. Plates also

available at https://doi.org/10.3133/pp235.] Benson, L., Madole, R., Landis, G., and Gosse, J., 2005, New data for late Pleistocene alpine glaciation from southwestern Colorado: Quaternary Science Reviews, v. 24, p. 46–65. [Also available at https://doi.org/10.1016/j.quascirev.2004.07.018.] Benson, L., Madole, R., Phillips, W., Landis, G., Thomas, T., and Kubic, P., 2004, The probable importance of snow and sediment shielding on cosmogenic ages of north-central Colorado Pinedale and pre-Pinedale moraines: Quaternary Science Reviews, v. 23, p. 193–206. [Also available at

https://doi.org/10.1016/j.quascirev.2003.07.002.] Bickford, M.E., Van Schmus, W.R., and Zietz, I., 1986, Proterozoic history of the midcontinent region of North America: Geology, v. 14, no. 6, p. 492–496. [Also available at https://doi.org/10.1130/0091-7613(1986)14%3C492:PHOTMR%3E2.0.CO;2. Birkeland, P.W., 1999, Soils and geomorphology: New York, Oxford University Press, 430 p. Bohannon, R.G., and Ruleman, C.A., 2013, Geologic map of the Mount Sherman 7.5' quadrangle, Lake and Park Counties, Colorado: U.S. Geological Survey Scientific Investigations Map 3271, scale 1:24,000, accessed Dec. 3, 2019, at

Boardman, S.J., and Condie, K.C., 1986, Early Proterozoic bimodal volcanic rocks in central Colorado, U.S.A., Part II, Geochemistry, petrogenesis and tectonic setting: Precambrian Research, v. 34, no. 1, p. 37–68. [Also available at https://doi.org/10.1016/0301-9268(86)90059-8.] Briner, J.P., 2009, Moraine pebbles and boulders yield indistinguishable <sup>10</sup>Be ages—A case study from Colorado, USA: Quaternary Geochronology, v. 4, no. 4, p. 299–305. [Also available at https://doi.org/10.1016/j.quageo.2009.02.010.] Brugger, K.A., 2007, Cosmogenic <sup>10</sup>Be and <sup>36</sup>Cl ages from late Pleistocene terminal

https://doi.org/10.3133/sim3271

moraine complexes in the Taylor River drainage basin, central Colorado, USA: Quaternary Science Reviews, v. 26, no. 3–4, p. 494–499. [Also available at https://doi.org/10.1016/j.quascirev.2006.09.006.] Cappa, J.A. and Bartos, P.J., 2007, Geology and mineral resources of Lake County, Colorado: Colorado Geological Survey, Resource Series 42, 58 p., scale 1:50,000. [Also available at https://store.coloradogeologicalsurvey.org/product/geology-mineral-resources-lake-colorado/.] Chamberlain, K.R., 1998, Medicine Bow orogeny—Timing of deformation and model of

crustal structure produced during continental-arc collision, ca. 1.78 Ga, southeastern Wyoming, in Karlstrom, K.E., ed., Introduction to special issues—Lithospheric structure and evolution of the Rocky Mountains (Parts 1 and 2): Rocky Mountain Geology, v. 33, no. 2, p. 259–277. [Also available at https://doi.org/10.2113/33.2.259.] Chapin, C.E., and Cather, S.M., 1983, Eocene tectonics and sedimentation in the Colorado Plateau–Rocky Mountain area, in Lowell, J.D., ed., Rocky Mountain foreland basins and uplifts, 1983 Symposium and Field Conference, Steamboat Springs, Colo., Oct. 3, 1983: Rocky Mountain Association of Geologists Proceedings and Guidebook, p. 33–56. [Also available at http://archives.datapages.com/data/rmag/ForelandBasinUp83/chapin.htm.]

Chapin C.F. and Kelley S.A. 1997. The Rocky Mountain erosion surface in the Front Range of Colorado, in Boyland, D.W., and Sonnenberg, S.A., eds., Colorado Front Range Guidebook–1997: Rocky Mountain Association of Geologists, p. 101–114. http://archives.datapages.com/data/rmag/geohistfrontrange1997/chapin\_b.htm.] Coe, J.A., Ruleman, C.A., Godt, J.W., Matthews, V., Goehring, B.M., Lucha, P., Deuell,

A.E., and Reeves, R.R., 2013, Long-term measurement of ridge-spreading movements (sakungen) at Bald Eagle Mountain, central Colorado [abs.]: Geological Society of America Abstracts with Programs, v. 45, no. 7, 643 p. [Also available at https://gsa.confex.com/gsa/2013AM/webprogram/Paper227500.html.] Cunningham, C.G., Naeser, C.W., Marvin, R.F., Luedke, R.G., and Wallace, A.R., 1994, Ages of selected intrusive rocks and associated ore deposits in the Colorado mineral belt: U.S. Geological Survey Bulletin 2109, 31 p. [Also available at https://doi.org/10.3133/b2109.]

De Voto, R.H., 1980, Pennsylvanian stratigraphy and history of Colorado, *in* Kent, H.C

and Porter, K.W., eds., Colorado geology: Rocky Mountain Association of Geologists Guidebook, p. 71–101. [Available at https://www.rmag.org/store/tangible-publications/the-rmag-library-1937-2001-dvd/?back=products.] Duebendorfer, E.M., and Houston, R.S., 1987, Proterozoic accretionary tectonics at the southern margin of the Archean Wyoming Craton: Geological Society of America Bulletin, v. 98, no. 5, p. 554–568. [Also available at https://doi.org/10.1130/0016-7606(1987)98%3C554:PATATS%3E2.0.CO;2.]

Curtis, B.F., ed., Cenozoic history of the Southern Rocky Mountains: Geological Society of America Memoirs, v. 144, p. 45–74, [Also available at https://doi.org/10.1130/MEM144-p45.] Frost, C.D., and Frost, B.R., 1997, Reduced rapakivi-type granites—The tholeiite connection: Geology, v. 25, p. 647–650. [Also available at https://doi.org/10.1130/0091-7613(1997)025%3C0647:RRTGTT%3E2.3.CO;2.] Frothingham, M.G., 2017, Metalamprophyre dike deformation in the Homestake Reservoir quadrangle, Leadville, Colorado: Bozeman, Montana State University, M.S. thesis, 144 p., accessed Dec. 3, 2019, at https://scholarworks.montana.edu/xmlui/handle/1/12778

Epis, R.C., and Chapin, C.E., 1975, Geomorphic and tectonic implications of the

post-Laramide, late Eocene erosion surface in the Southern Rocky Mountains, in

Gosse, J.C., and Phillips, F.M., 2001, Terrestrial in situ cosmogenic nuclides—Theory and application: Quaternary Science Reviews, v. 20, no. 14, p. 1475–1560. [Also available at https://doi.org/10.1016/S0277-3791(00)00171-2.] Guido, Z.S., Ward, D.J., and Anderson, R.S., 2007, Pacing the post-Last Glacial Maximum demise of the Animas Valley glacier and the San Juan ice cap, Colorado: Geology, v. 35, no. 8, p. 739–742. [Also available at https://doi.org/10.1130/G23596A.1.] Holm, D., Schneider, D., and Coath, C.D., 1998, Age and deformation of early Proterozoic quartzites in the southern Lake Superior region—Implications for extent

of foreland deformation during final assembly of Laurentia: Geology, v. 26, no. 10, p. 907–910. [Also available at https://doi.org/10.1130/0091-7613(1998)026%3C0907:AADOEP%3E2.3.CO;2.] Houck, K.J., Funk, J.A., Kirkham, R.M., Carroll, C.J., and Heberton-Morimoto, A.D., 2012, Marmot Peak quadrangle geologic map, Park and Chaffee Counties, Colorado: Colorado Geological Survey Open File Report OF–12–07, scale 1:24,000. [Also available at https://store.coloradogeologicalsurvey.org/product/geologic-mapmarmot-peak-quadrangle-chaffee-park-colorado/.]

Houston, R.S., Duebendorfer, E.M., Karlstrom, K.E., and Premo, W.R., 1989, A review of the geology and structure of the Cheyenne Belt and Proterozoic rocks of southern Wyoming, in Grambling, J.A., and Tewksbury, B.J., eds., Proterozoic geology of the Southern Rocky Mountains: Boulder, Colo., Geological Society of America Special Paper, v. 235, p. 1–12. [Also available at https://doi.org/10.1130/SPE235-p1.] Karlstrom, K.E., and Bowring, S.A., 1988, Early Proterozoic assembly of tectonostratigraphic terranes in southwestern North America: Journal of Geology, v. 96, no. 5, p. 561–576. [Also available at https://doi.org/10.1086/629252.] Karlstrom, K.E., and Houston, R.S., 1984, The Cheyenne belt; analysis of a Proterozoic suture in southern Wyoming: Precambrian Research, v. 25, p. 415–446. [Also

available at https://doi.org/10.1016/0301-9268(84)90012-3.] Kellogg, K.S., Shroba, R.R., Bryant, B., and Premo, W.R., 2008, Geologic map of the Denver West 30'×60' quadrangle, north-central Colorado: U.S. Geological Survey Scientific Investigations Map 3000, pamphlet 48 p., scale 1:100,000. [Also available at https://doi.org/10.3133/sim3000. Kellogg, K.S., Shroba, R.R., Premo, W.R., and Bryant, B., 2011, Geologic map of the

eastern half of the Vail 30'×60' quadrangle, Eagle, Summit, and Grand Counties, Colorado: U.S. Geological Survey Scientific Investigations Map 3170, pamphlet 49 p., scale 1:100,000. [Also available at https://doi.org/10.3133/sim3170.] Kellogg, K.S., Shroba, R.R., Ruleman, C.A., Bohannon, R.G., McIntosh, W.C., Premo. W.R., Cosca, M.A., Moscati, R.J., and Brandt, T.R., 2017, Geologic map of the upper Arkansas River valley region, north-central Colorado: U.S. Geological Survey Scientific Investigations Map 3382, pamphlet 70 p., 2 sheets, scale 1:50,000,

accessed Dec. 3, 2019, at https://doi.org/10.3133/sim3382 Kirkham, R.M., Houck, K.J., Carroll, C.J., and Heberton-Morimoto, A.D., 2012, Geologic map of the Antero Reservoir quadrangle, Park and Chaffee Counties, Colorado: Colorado Geological Survey Open File Report OF–12–01, scale 1:24,000. [Also available at https://data.colorado.gov/State/OF-12-01-Geologic-Map-of-the-Antero-Reservoir-Quad/77aa-c5gh.]

Kirkham, R.M., Keller, J.W., Houck, K.J., and Lindsay, N.R., 2006, Geologic map of the Fairplay East quadrangle, Park County, Colorado: Colorado Geological Survey Open File Report OF-06-09, scale 1:24,000. [Also available at https://store.coloradogeologicalsurvey.org/product/geologic-map-fairplay-east-quadr angle-park-colorado/.] Lal, D., 1991, Cosmic ray labeling of erosion surfaces—In-situ nuclide production rates and erosion models: Earth and Planetary Science Letters, v. 104, p. 424–439. [Also available at https://doi.org/10.1016/0012-821X(91)90220-C.] Lee, P.E., Jessup, M.J., Shaw, C.A., Hicks, G.L., and Allen, J.L., 2012, Strain partitioning in the mid-crust of a transpressional shear zone system—Insights from the

Homestake and Slide Lake shear zones, central Colorado: Journal of Structural Geology, v. 39, p. 237–252. [Also available at https://doi.org/10.1016/j.jsg.2012.02.006.] Leonard, E.M., Laabs, B.J.C., Schweinsberg, A.D., Russell, C.M., Briner, J.P., and Young, Nicolás, 2017, Deglaciation of the Colorado Rocky Mountains following the Last Glacial Maximum: Cuadernos de Investigación Geográfica, v. 43, no. 2, p. 497–526, accessed January 28, 2020, at https://doi.org/10.18172/cig.3234. Lisiecki, L.E., and Raymo, M.E., 2005, A Pliocene-Pleistocene stack of 57 globally distributed benthic  $\delta^{18}$ O records: Paleoceanography, v. 20, no. 1, 17 p., accessed Dec. 3, 2019, at https://doi.org/10.1029/2004PA001071.

Mach, C.J., 1992, Geology and mineral deposits of the Kokomo District: Fort Collins, Colo., Colorado State University, M.S. thesis, 154 p. Madole, R.F., 1986, Lake Devlin and Pinedale glacial history, Front Range, Colorado: Ouaternary Research, v. 25, p. 43–54. [Also available at https://doi.org/10.1016/0033-5894(86)90042-6.]

Marvin, R.F., Mehnert, H.H., Naeser, C.W., and Zartman, R.E., 1989, U.S. Geological Survey radiometric ages—Compilation "C" part five—Colorado, Montana, Utah, and Wyoming: Isochron/West, no. 53, p. 14–19. [Available through the New Mexico Bureau of Geology and Mineral Resources. Mason, C., Ruleman, C.A., and Kenny, R., 2011, Rate and timing of deglaciation using

<sup>o</sup>Be cosmogenic nuclide surface exposure dating, Mt. Massive Wilderness Colorado, USA [abs.]: Geological Society of America Abstracts with Programs v. 43, no. 5, 65 p. [Also available at https://gsa.confex.com/gsa/2011AM/finalprogram/abstract\_193344.htm.] McCalpin, J.P., Temple, J., Sicard, K., Mendel, D., and Ahmad, B., 2012, Climax quadrangle geologic map, Lake and Park Counties, Colorado: Colorado Geologica Survey Open File Report OF-12-09, scale 1:24,000. [Also available at https://data.colorado.gov/State/OF-12-09-Geologic-Map-of-the-Climax-Quadrangle-Lak/v2pt-ybqy.]

McCoy, A.M., Karlstrom, K.E., Shaw, C.A., and Williams, M.L., 2005, The Proterozoic ancestry of the Colorado mineral belt—1.4 Ga shear zone system in central Colorado in Karlstrom, K.E., and Keller, G.R., eds., The Rocky Mountain region, an evolving lithosphere—Tectonics, geochemistry, and geophysics: American Geophysical Union, v. 154, p. 71–90. [Also available at https://doi.org/10.1029/154GM06.] Meierding, T.C., and Birkeland, P.W., 1980, Quaternary glaciation of Colorado, in Kent, H.C., and Porter, K.W., eds., Colorado geology: Denver, Rocky Mountain Association of Geologists Guidebook, p. 165–173. [Also available at https://www. rmag.org/store/tangible-publications/the-rmag-library-1937-2001-dvd/?back=products.] Merson, M.Q., Allen, J.L., and Shaw, C.A., 2015, Metamorphosed and mylonitic

pseudotachylytes from the Homestake and Slide Lake shear zones, Colorado, USA in T38, Sigma Gamma Epsilon—Undergraduate research, 2015 GSA Annual Meeting, Baltimore, Md., November 1–4, 2015 [posters]: Geological Society of America Abstracts with Programs, v. 47, no. 7, 529 p., accessed Dec. 3, 2019, at https://gsa.confex.com/gsa/2015AM/webprogram/Paper259825.html. Morozova, E., Wan, X., Chamberlain, K.R., Smithson, S.B., Morozov, I.B., Boyd, N.K.. Johnson, R.A., Karlstrom, K.E., Tyson, A.R., and Foster, C.T., 2002, Geometry of Proterozoic sutures in the Central Rocky Mountains from seismic reflection data— Cheyenne Belt and Farwell Mountain structures: Geophysical Research Letters, v. 29 no. 13, p. 17-1–17-4. [Also available at https://doi.org/10.1029/2001GL013819.] Moscati, R.J., Premo, W.R., DeWitt, E.H., and Wooden, J.L., 2017, U-Pb ages and Ranges, Colorado, U.S.A.—Implications for crustal growth of the central Colorado

geochemistry of zircon from Proterozoic plutons of the Sawatch and Mosquito province: Rocky Mountain Geology, v. 52, no. 1, p. 17–106, accessed Dec. 3, 2019, at https://doi.org/10.24872/rmgjournal.52.1.1 Myrow, P.M., Taylor, J.F., Miller, J.F., Ethington, R.L., Ripperton, R.L., and Allen, J., 2003, Fallen arches—Dispelling myths concerning Cambrian and Ordovician paleogeography of the Rocky Mountain region: Geological Society of America Bulletin, v. 115, no. 6, p. 695–713. [Also available at https://doi.org/10.1130/0016-7606(2003)115%3C0695:FADMCC%3E2.0.CO;2.] Nelson, A.R., and Shroba, R.R., 1998, Soil relative dating of moraine and outwash-terrace sequences in the northern part of the upper Arkansas Valley, central

Colorado, U.S.A.: Arctic and Alpine Research, v. 30, no. 4, p. 349–361. [Also available at https://doi.org/ 10.2307/1552007.] Pearson, R.C., Tweto, O., Stern, T.W., and Thomas, H.H., 1962, Age of Laramide porphyries near Leadville, Colorado, in Short papers in geology, and hydrology Articles 60–119: U.S. Geological Survey Professional Paper 450–C, p. C78–C80 [Also available at https://doi.org/10.3133/pp450C.] Premo, W.R., Kellogg, K.S., Bryant, B., 2007, SHRIMP U-Pb zircon ages for Paleoproterozoic basement rocks from the northern and central Colorado Front Range—A refinement of the timing of crustal growth in the Colorado Province, in Precambrian Geology, 2007 GSA Annual Meeting, Denver, Colo., October 28–31, 2007 [posters]: Geological Society of America Abstracts with Programs, v. 39, no. 6, 221 p. [Also available at https://gsa.confex.com/gsa/2007AM/finalprogram/abstract\_130581.htm.] Reed, J.C., Jr., Bickford, M.E., and Tweto, O., 1993, Proterozoic accretionary terranes of Colorado and southern Wyoming, in Van Schmus, W.R., and Bickford, M.E., eds., Transcontinental Proterozoic provinces, in Reed, J.C., Jr., Bickford, M.E., Houston,

R.S., Link, P.K., Rankin, D.W., Sims, P.K., and Van Schmus, W.R., eds., The geology of North America, Precambrian—Conterminous U.S.: Geological Society of America, v. C-2, p. 211–228. [Also available at https://doi.org/10.1130/DNAG-GNA-C2.171.] Richmond, G.M., and Fullerton, D.S., 1986, Introduction to Quaternary glaciations in the United States of America, Richmond, G.M., and Fullerton, D.S., eds., Quaternary glaciations in the United States of America: Quaternary Science Reviews, v. 5, Rock, N.M., 1987, The nature and origin of lamprophyres—An overview: London, Geological Society Special Publications, v. 30, no. 1, p. 191–226. [Also available at https://doi.org/10.1144/GSL.SP.1987.030.01.09.] Ruleman, C.A., Bohannon, R.G., Bryant, B., Shroba, R.R., and Premo, W.R., 2011, Geologic map of the Bailey 30'×60' quadrangle, north-central Colorado: U.S.

Geological Survey Scientific Investigations Map 3156, pamphlet 38 p., scale 1:100,000. [Also available at https://doi.org/10.3133/sim3156.] Ruleman, C.A., Brandt, T.R., Caffee, M.W., and Goehring, B.M., 2018, Geologic map of the Leadville North 7.5' quadrangle, Eagle and Lake Counties, Colorado: U.S. Geological Survey Scientific Investigations Map 3400, scale 1:24,000, accessed Dec. 3, 2019, at https://doi.org/10.3133/sim3400.] Ruleman, C.A., Goehring, B.M., Mason, C., and Lundstrom, S.C., 2013, Late Pleistocene glacial maximum and deglaciation of the northern Sawatch Range, Mount Massive Colorado [abs.]: Geological Society of America Abstracts with Programs, v. 45, no. 7,

551 p. [Also available at https://gsa.confex.com/gsa/2013AM/webprogram/Paper231017.html.] Ruleman, C., and Hudson, A.M., 2016, The Central Colorado Icefield, a mechanism for inception of regional exhumation and deep-canyon incision during the Pleistocene? [abs.]: Geological Society of America Abstracts with Programs, v. 48, no. 7. [Also available at https://doi.org/10.1130/abs/2016AM-282920.] Ruleman, C., Hudson, A.M., Caffee, M.W., and Brugger, K.A., 2018, MIS 12-11 (478–374 ka) ~middle Pleistocene glaciation of the central and southern Rocky Mountain-Colorado Plateau region—Links to landscape evolution of major western

North American rivers [abs.]: Geological Society of America Abstracts with Programs, v. 50, no. 5. [Also available at https://doi.org/10.1130/abs/2018RM-314061.] Ruleman, C., Hudson, A.M., Caffee, M.W., and Brugger, K.A., 2019a, The middle Pleistocene unconformity and MIS 12–11 (~478–385 ka)—Glaciofluvial processes override late Miocene-middle Pleistocene (~6 Ma-500 ka) tectono-magmatic capture and deep-canyon incision, western Great Plains-southern Rocky Mountains-Colorado Plateau region, North America [abs.]: Geological Society of America Abstracts with Programs, v. 51, no. 5, [Also available at

https://doi.org/10.1130/abs/2019AM-339129.] Ruleman, C., Hudson, A.M., Caffee, M.W., Goehring, B.M., Sortor, R.N., Brugger, K.A. Frothingham, M.G., and Nicovich, S.R., 2019b, MIS 12–11 (478–374 ka) ~ middle Pleistocene glaciation of the southern Rocky Mountain-Great Plain region—Links to landscape evolution of major central North American rivers [abs.]: Geological Society of America Abstracts with Programs, v. 51, no. 2. [Also available at https://doi.org/10.1130/abs/2019SC-326957.]

Schildgen, T., Dethier, D.P., Bierman, P., and Caffee, M., 2002, <sup>26</sup>Al and <sup>10</sup>Be dating of late Pleistocene and Holocene fill terraces—A record of fluvial deposition and incision, Colorado Front Range: Earth Surface Processes and Landforms, v. 27, no. 7, p. 773–787. [Also available at https://doi.org/10.1002/esp.352.] Shaw, C.A., and Allen, J.L., 2007, Field rheology and structural evolution of the Homestake shear zone, Colorado: Rocky Mountain Geology, v. 42, no. 1, p. 31–56. [Also available at https://doi.org/10.2113/gsrocky.42.1.31.] Shaw, C.A., Heizler, M.T., Karlstrom, K.E., and Keller, G.R., 2005, 40Ar/39Ar thermo-

chronologic record of 1.45–1.35 Ga intracontinental tectonism in the southern

Rocky Mountains—Interplay of conductive and advective heating with intracontinental deformation, in Karlstrom, K.E., and Keller, R.G., eds., The Rocky Mountain Region—An evolving lithosphere: American Geophysical Union Geophysical Monograph Series, v. 154, p. 163–184. [Also available at https://doi.org/10.1029/154GM12.] Shaw, C.A., Karlstrom, K.E., Williams, M.L., Jercinovic, M.J., and McCoy, A.M., 2001, Electron-microprobe monazite dating of ca. 1.71–1.63 Ga and ca. 1.45–1.38 Ga deformation in the Homestake shear zone, Colorado—Origin and early evolution of a persistent intracontinental tectonic zone: Geology, v. 29, no. 8, p. 739–742. [Also available at https://doi.org/10.1130/0091-7613(2001)029%3C0739:EMMDOC%3E2.0.CO;2.] Silver, L.T., 1965, Mazatzal orogeny and tectonic episodicity [abs.], in Abstracts of papers submitted for six meetings with which the Society was associated, Miami Beach, Florida, November 19–21, 1964: Geological Society of America Special

Silver, L.T., 1967, Apparent age relations in the older Precambrian stratigraphy in Arizona [abs.], in Burwash, R.A., and Morton, R.D., eds., Geochronology of Precambrian Stratified Rock: Edmonton, Alberta, University of Alberta, Conference of June 1967, 87 p. [Available from the University of Alberta Library, call no. QE 655 C742 1967.1 Silver, L.T., 1969, Precambrian batholiths of Arizona [abs.], in Abstracts of papers submitted for seven meetings with which the Society was associated, for the meeting in Tucson, Arizona April 11–13, 1968—Cordilleran Section, Geological Society of America, the Seismological Society, The Paleontological Society, Pacific Coast

Paper, v. 82, p. 185–186. [Also available at https://doi.org/10.1130/SPE82-p1.]

Section: Geological Society of America Special Paper, v. 121, p. 558–559. [Also available at https://doi.org/10.1130/SPE121-p477.] Silver, L.T., Bickford, M.E., Van Schmus, W.R., Anderson, J.L., Anderson, T.H., and Medaris, L.G., Jr., 1977, The 1.4–1.5 b.y. transcontinental anorogenic plutonic perforation of North America [abs.]: Geological Society of America Abstracts with Programs, v. 9, p. 1176–1177.

Stark, J.T., and Barnes, F.F., 1935, Geology of the Sawatch Range, Colorado: Colorado Scientific Society Proceedings, v. 13, p. 470–474. Stone, J.O., 2000, Air pressure and cosmogenic isotope production: Journal of Geophysical Research Solid Earth, v. 105, no. B10, p. 23753–23759. [Also available at https://doi.org/10.1029/2000JB900181.] America Bulletin, v. 62, p. 507–532.

Tweto, O., 1951, Form and structure of sills near Pando, Colorado: Geological Society of Tweto, O., 1974, Geologic map and sections of the Holy Cross quadrangle, Eagle, Lake, Pitkin, and Summit Counties, Colorado: U.S. Geological Survey Miscellaneous Investigations Series Map I–830, 2 sheets, scale 1:24,000 [Brandt, T.R., Digital edition, 2013]. [Also available at https://doi.org/10.3133/i830.] Tweto, O., 1975, Laramide (Late Cretaceous–early Tertiary) orogeny in the Southern Rocky Mountains, in Curtis, B.F., ed., Cenozoic history of the Southern Rocky Mountains, Geological Society of America Memoirs, v. 144, p. 1–44. [Also available at https://doi.org/10.1130/MEM144-p1.

Tweto, O., 1979, The Rio Grande rift system in Colorado, in Riecker, R.E., ed., Rio Grande Rift—Tectonics and Magmatism: American Geophysical Union Special Publications, v. 14, p. 33–56. [Also available at https://doi.org/10.1029/SP014p0033.] Tweto, O., 1987, Geology of the Precambrian basement in Colorado—Rock units of the Precambrian basement in Colorado: U.S. Geological Survey Professional Paper 1321–A, pamphlet 54 p., 1 pl., scale 1:1,000,000. [Also available at https://doi.org/10.3133/pp1321A.] Tweto, O., and Pearson, R.C., 1964, St. Kevin Granite, Sawatch Range, Colorado, in Geological Survey Research 1963—Short papers in geology and hydrology, Articles

122–172: U.S. Geological Survey Professional Paper 475–D, p. D28–D32. [Also available at https://doi.org/10.3133/pp475D. Tweto, O., and Sims, P.K., 1963, Precambrian ancestry of the Colorado mineral belt: Geological Society of America Bulletin, v. 74, no. 8, p. 991–1014. [Also available at https://doi.org/10.1130/0016-7606(1963)74[991:PAOTCM]2.0.CO;2.] Tyson, A.R., Morozova, E.A., Karlstrom, K.E., Chamberlain S.B., Smithson K.G. Dueker, K.R., and Foster, C.T., 2002, Proterozoic Farwell Mountain—Lester Mountain suture zone, northern Colorado—Subduction flip and progressive assembly of arcs: Geology, v. 30, no. 10, p. 943–946. [Also available at https://doi.org/10.1130/0091-7613(2002)030%3C0943:PFMLMS%3E2.0.CO;2.]

University of Washington, 2019, CRONUS-Earth online calculator ver. 2.2: Seattle, Wash., Cosmogenic Nuclide Lab, University of Washington, accessed Dec. 2, 2019, at https://hess.ess.washington.edu/. U.S. Geological Survey Geologic Names Committee, 2018, Divisions of geologic time—Major chronostratigraphic and geochronologic units: U.S. Geological Survey Fact Sheet 2018–3054, 2 p., https://doi.org/10.3133/fs20183054. Varnes, D.J., Radbruch-Hall, D.H., Varnes, K.L., Smith, W.K., and Savage, W.Z., 1990,

Measurement of ridge-spreading movements (sackungen) at Bald Eagle Mountain, Lake County, Colorado, 1975–1989: U.S. Geological Survey Open-File Report 90–543, 13 p. [Also available at https://doi.org/10.3133/ofr90543.] Wallace, A.R., 1993, Geologic setting of the Leadville mining district, Lake County, Colorado: U.S. Geological Survey Open-File Report 93–343, 19 p. [Also available at https://doi.org/10.3133/ofr93343.] Ward, D.W., Anderson, R.S., Briner, J.P., and Guido, Z.S., 2009, Numerical modeling of cosmogenic deglaciation records, Front Range and San Juan Mountains, Colorado: Journal of Geophysical Research: Earth Surface, v. 114, no. F1, F01026 p. [Also

available at http://doi.org/10.1029/2008JF001057.] White, S.E., 1971, Rock glacier studies in the Colorado Front Range, 1961 to 1968: Arctic and Alpine Research, v. 3, no. 1, p. 43–64. [Also available at https://www.tandfonline.com/doi/abs/10.1080/00040851.1971.12003596.] White, S.E., 1976, Rock glaciers and block fields, review and new data: Quaternary Research, v. 6, no. 1, p. 77–97. [Also available at https://doi.org/10.1016/0033-5894(76)90041-7.] Whitmeyer, S.J., and Karlstrom, K.E., 2007, Tectonic model for the Proterozoic growth of North America: Geosphere, v. 3, no. 4, p. 220–259. [Also available at

Young, N.E., Briner, J.P., Leonard, E.M., Licciardi, J.M., and Lee, K., 2011, Assessing climatic and nonclimatic forcing of Pinedale glaciation and deglaciation in the western US: Geology, v. 39, no. 2, p. 171–174. [Also available at https://doi.org/10.1130/G31527.1.]

Suggested citation: Ruleman, C.A., Frothingham, M.G., Brandt, T.R., Shaw, C.A., Caffee, M.W., Brugger, K.A., and Goehring,

Associated data for this publication: Ruleman, C.A., Frothingham, M.G., Brandt, T.R., Shaw, C.A., Caffee, M.W., Brugger, K.A.

Goehring, B.M., 2020, Data release for geologic map of the Homestake Reservoir quadrangle, Colorado: U.S. Geological Survey

B.M., 2020, Geologic map of the Homestake Reservoir 7.5' quadrangle, Lake, Pitkin, and Eagle Counties, Colorado: U.S

Geological Survey Scientific Investigations Map 3451, scale 1:24,000, https://doi.org/10.3133/sim3451.

https://doi.org/10.1130/GES00055.1.

Report digital files available at https://doi.org/10.3133/sim3451

Geologic Map of the Homestake Reservoir 7.5' Quadrangle, Lake, Pitkin, and Eagle Counties, Colorado

<sup>1</sup>U.S. Geological Survey

2013; Merson and others, 2015).